arXiv:1106.5838v1 [cond-mat.mes-hall] 29 Jun 2011

Excitonic condensation in the topological insulator bilayer systems: A self-consistent mean-field theory study

Zhigang Wang,[1] Ningning Hao,[2,1] Zhen-Guo Fu,[3,1] and Ping Zhang[1,*]
[1]*LCP, Institute of Applied Physics and Computational Mathematics,*
P.O. Box 8009, Beijing 100088, People's Republic of China
[2]*Institute of Physics, Chinese Academy of Sciences, Beijing 100080, People's Republic of China*
[3]*State Key Laboratory for Superlattices and Microstructures,*
Institute of Semiconductors, Chinese Academy of Sciences,
P. O. Box 912, Beijing 100083, People's Republic of China

We propose a generic topological insulator bilayer (TIB) system to study the excitonic condensation with self-consistent mean-field (SCMF) theory. We show that the TIB system presents the crossover behavior from the Bardeen-Cooper-Schrieffer (BCS) in weak coupling limit to Bose-Einstein condensation (BEC) in the strong coupling limit in zero temperature limit. Moreover, comparing to those in the traditional semiconductor systems, we find that the superfluid property in the BEC phase is more sensitive to electron-hole density imbalance and the BCS phase is more robust in the weak coupling limit. Applying this TIB model into Bi_2Se_3 material, we find that only the BEC phase can be observed in experiment. We also calculate the critical temperature for Bi_2Se_3TIB system and find that is about 100 K. More interestingly, we can expect the relative high-temperature excitonic condensation since the Kosterlitz-Thouless transition does not suppress the critical temperature for Bi_2Se_3 in SCMF approximation.

PACS numbers: 73.21.Fg, 73.20.Mf, 71.10.Li

I. INTRODUCTION

Recent technological advances in microfabrication bring growing interests in studying exciton condensation in different bilayer physical systems such as the semiconductor electron-hole bilayer [1–3] and graphene bilayer [4, 5]. A number of novel physical phenomena are obtained in these systems, such as the BCS-BEC crossover [6] as well as the subtle phase transition in the crossover region induced by the density imbalance [7], the dark and bright excitonic condensation under spin-orbit coupling [8], anomalous exciton condensation in high Landau levels in magnetic field [5], room-temperature superfluidity in graphene bilayer [9], etc. The conventional electron-hole bilayer is fabricated with semiconductor such as GaAs/AlGaAs/GaAs. The character of the semiconductor electron-hole bilayer systems is that the electron and hole bands are quadratic ones with different effective masses, which means missing particle-hole symmetry in these kinds of systems and weak stiff phase order. Hence, in semiconductor electron-hole bilayers, the excitonic condensation needs very low temperature. Another better candidate for electron-hole bilayers is graphene, which has two-dimensional massless linear Dirac-band structure in low energy limit. However, the coupling between different Dirac-cone structures in the same Brilliouin zone brings flaw to graphene to fabricate electron-hole bilayer [10].

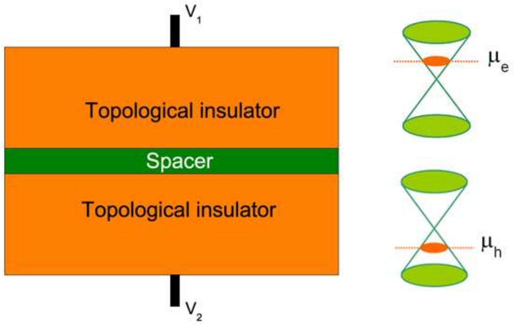

FIG. 1: (Color online) Left panel: Schematic structure of double-well topological insulators in x-y plane. The external gates can independently tune the electron and hole densities. Right panel: The linear energy dispersion around the Dirac point of the electrons and holes.

On the other hand, another growing interest in condensed matter physics is the very recent theoretical prediction [11, 12] and experimental verification [13] of the topological insulators (TIs) with strong spin-orbit interaction. Several three-dimensional (3D) solids, such as $Bi_{1-x}Sb_x$ alloys, Bi_2Se_3-family crystals, have been identified [14–18] to be strong TIs possessing anomalous band structures. The energy scale for the surface states of these 3D TIs is dominated by the k-linear spin-orbit interaction instead of the k-quadratic ones even as that in semiconductor. Especially, the strong TIs surface has single Dirac-cone band structure which is also different from graphene. As a result, it is expected that the excitonic condensate of these topological surface states probably have new characters.

Inspired by this expectation, as well as by the recent experimental access to high-quality TI quantum well

---

[*] Corresponding author. Email address: zhang_ping@iapcm.ac.cn

films on insulating substrate [19], in this paper we propose a TIB model, a gated double TI layers separated by an insulating spacer. Using this TIB model, we theoretically study the excitonic condensation of these surface states. We find that the system also presents BCS-BEC crossover along with change of the carriers densities in zero temperature limit. However, there are two characters different from those of conventional excitonic condensation in semiconductor bilayer systems. The first is that the BCS phase of TIB is more robust than that of the semiconductor bilayer in weak coupling limit; the second is that the superfluidity of the TIB is more sensitive to the carriers densities imbalance than that of the semiconductor bilayer in strong coupling limit. These two characters physically root in the k-linear band dispersion of the TIB. Moreover, by putting this TIB model in $\mathrm{Bi_2Se_3}$ material, we investigate the excitonic condensation in the $\mathrm{Bi_2Se_3}$ bilayer and only find the BEC phase occurring due to the values of the parameters of the material. The critical temperature of excitonic condensation in $\mathrm{Bi_2Se_3}$ TIB ($\sim$ 100 K) is also calculated in the self-consistent mean-field (SCMF) approximation, which is found to be higher than that in the traditional semiconductor electron-hole bilayers. More interestingly, we can expect the relative high-temperature excitonic condensation since the KT transition does not suppress the critical temperature for $\mathrm{Bi_2Se_3}$ in SCMF approximation.

II. THE TIB MODEL

The TIB model is schematically illustrated in the left panel of Figure 1. Two TI films are separated by an insulating spacer of thickness d, and the electron (hole) density can be independently tuned by the external gate voltage V_1 (V_2). The linear dispersions of the TIs around Dirac points are cartoonishly depicted in the right panel of Figure 1. A similar setup has been proposed by Zhu et al. [3] for the conventional semiconductor system. The only difference is that the two semiconductor quantum wells are now replaced by the two TI films. However, this replacement changes the energy dispersion of the electrons (holes) and raises different physical properties.

The grand-canonical Hamiltonian describing this TIB system can be written as

$$\begin{aligned} H = & \sum_{\mathbf{k},\sigma} \left(\epsilon_{\mathbf{k}\sigma} - \mu_\sigma\right) c^\dagger_{\mathbf{k}\sigma} c_{\mathbf{k}\sigma} + \frac{1}{2\Omega} \qquad (1) \\ & \times \sum_{\substack{\mathbf{k},\mathbf{k}',\mathbf{q} \\ \sigma,\sigma'}} V^{\sigma\sigma'}_{\mathbf{k}-\mathbf{k}'} c^\dagger_{\mathbf{k}+\mathbf{q}/2\sigma} c^\dagger_{-\mathbf{k}+\mathbf{q}/2\sigma'} c_{-\mathbf{k}'+\mathbf{q}/2\sigma'} c_{\mathbf{k}'+\mathbf{q}/2\sigma}. \end{aligned}$$

Here, $\mathbf{k}$, $\mathbf{k}'$, and $\mathbf{q}$ are 2D wave vectors in the layers, Ω is the quantization volume, $c^\dagger_{\mathbf{k}\sigma}$ ($c_{\mathbf{k}\sigma}$) are the creation (annihilation) operator for an electron in electron (e) layer or hole (h) layer distinguished by σ=(e, h). The surface states of the strong TI film have the linear dispersion: $\epsilon_{\mathbf{k}e,h}=\pm\hbar v_F|\mathbf{k}|$ and μ_σ are chemical potentials for electron layer or hole layer. $V^{\sigma\sigma'}_{\mathbf{k}-\mathbf{k}'}$ is the Fourier transform of the Coulomb interaction: the intralayer Coulomb repulsive interaction $V^{ee}_{\mathbf{q}}(V^{hh}_{\mathbf{q}})=2\pi e^2/(q\varepsilon)$, and the interlayer Coulomb attractive interaction $V^{eh}_{\mathbf{q}}=-2\pi e^2\exp(-qd)/(q\varepsilon)$. Here, ε is the background dielectric constant and d is width of the spacer.

With the SCMF theory, Eq. (1) can be rewritten in a 2×2 matrix in the basis $(e,h)^T$, the relevant mean-field equations to be solved for the variables μ_e, μ_h, and the gap function $\Delta_{\mathbf{k}}$ are

$$\Delta_{\mathbf{k}} = -\frac{1}{\Omega}\sum_{\mathbf{k}'} V^{eh}_{\mathbf{k}-\mathbf{k}'} \frac{\Delta_{\mathbf{k}'}}{2E_{\mathbf{k}'}} \left[f(E^+_{\mathbf{k}'}) - f(E^-_{\mathbf{k}'})\right], \qquad (2)$$

$$\Sigma^e_{\mathbf{k}} = \frac{1}{\Omega}\sum_{\mathbf{k}'} V^{ee}_{\mathbf{k}-\mathbf{k}'} \left[u^2_{\mathbf{k}} f(E^+_{\mathbf{k}'}) + v^2_{\mathbf{k}} f(E^-_{\mathbf{k}'})\right], \qquad (3)$$

$$\Sigma^h_{\mathbf{k}} = \frac{1}{\Omega}\sum_{\mathbf{k}'} V^{hh}_{\mathbf{k}-\mathbf{k}'} \left[v^2_{\mathbf{k}} f(E^+_{\mathbf{k}'}) + u^2_{\mathbf{k}} f(E^-_{\mathbf{k}'})\right], \qquad (4)$$

$$n_e = \frac{1}{\Omega}\sum_{\mathbf{k}} \left\{u^2_{\mathbf{k}} f(E^+_{\mathbf{k}}) + v^2_{\mathbf{k}}\left[f(E^-_{\mathbf{k}})\right]\right\}, \qquad (5)$$

$$n_h = \frac{1}{\Omega}\sum_{\mathbf{k}} \left\{u^2_{\mathbf{k}}[1 - f(E^-_{\mathbf{k}})\} + v^2_{\mathbf{k}}\left[1 - f(E^+_{\mathbf{k}})\right]\right\}, \qquad (6)$$

where $f\left(E^\pm_{\mathbf{k}}\right)=1/(1+e^{E^\pm_{\mathbf{k}}/k_BT})$ is the Fermi-Dirac distribution function, $E_{\mathbf{k}}=\sqrt{\xi^2_{\mathbf{k}}+\Delta^2_{\mathbf{k}}}$ with $\xi_{\mathbf{k}}=\frac{1}{2}\left(\xi_{\mathbf{k}e}-\xi_{\mathbf{k}h}\right)$, $\xi_{\mathbf{k}\sigma}=\epsilon_{\mathbf{k}\sigma}-\mu_\sigma+\Sigma^\sigma_{\mathbf{k}}$ (σ=e, h), and $E^\pm_{\mathbf{k}}=\delta\xi_{\mathbf{k}}\pm E_{\mathbf{k}}$ with $\delta\xi_{\mathbf{k}}=\frac{1}{2}\left(\xi_{\mathbf{k}e}+\xi_{\mathbf{k}h}\right)$. In addition, $u^2_{\mathbf{k}}=1-v^2_{\mathbf{k}}=\frac{1}{2}\left(1+\xi_{\mathbf{k}}/E_{\mathbf{k}}\right)$. In two dimensions the average interparticle spacing is given by [7]

$$r_s = \frac{1}{\sqrt{\frac{\pi}{2}\left(n_e+n_h\right)}}. \qquad (7)$$

III. NUMERICAL RESULTS AND APPLICATION TO THE BI$_2$SE$_3$ MATERIAL

Many meaningful physical quantities can be obtained by self-consistent solving Eqs. (2)–(6). The exciton's energy spectrum is shown in Fig. 2(a) with parameters r_s=5 and α=0 in zero temperature limit. The corresponding density of states is shown in Fig. 2(b). A stable energy gap protecting the excitonic condensation is evident. Moreover, the wave-vector dependence of $\Delta_{\mathbf{k}}$ for equal densities and several values of r_s is shown in Fig. 3. We can find the generic feature of the BCS-BEC crossover behavior similar to that in the semiconductor bilayers. However, the striking character in the TI bilayers is that the maximum of $\Delta_{\mathbf{k}}$ in the weak coupling limit is much stronger than in the traditional semiconductor electron-hole bilayers [7]. The difference means the BCS phase of TIB is more robust than that of the semiconductor bilayer in weak coupling limit for equal densities case.

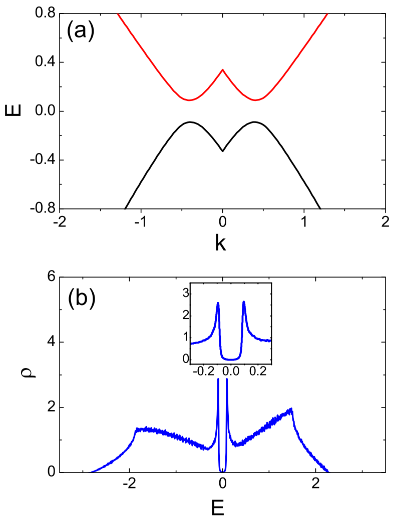

FIG. 2: (Color online) (a) Energy spectrum and (b) density of states of the exciton's system with r_s=5 and α=0. We choose $\hbar v_F$ as the energy unit and nm as the length unit. The diploe constant and the spacer width are set as ε=d=1.

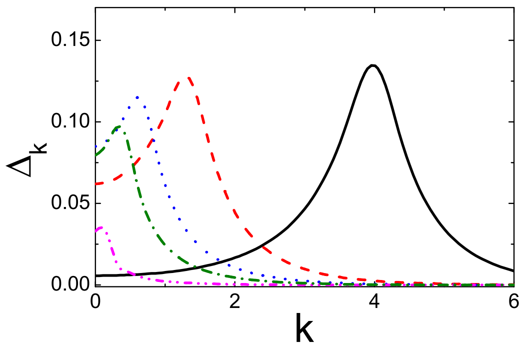

FIG. 3: (Color online) Wave-vector dependence of the gap function $\Delta_{\mathbf{k}}$ for α=0, d=1, and several values of r_s. The solid, dashed, dotted, dash-dotted, dash-dot-dotted lines are corresponding to r_s=0.5, 1.5, 3.0, 5.0, and 20.0, respectively.

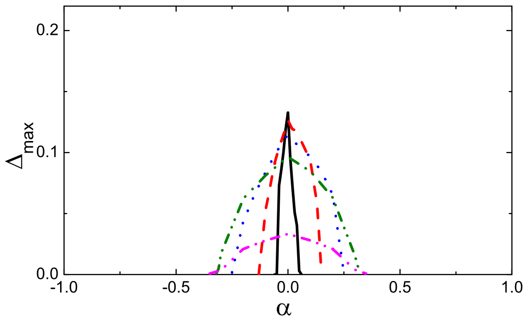

FIG. 4: (Color online) Maximum value $\Delta_{\max}$=max$\{\Delta_{\mathbf{k}}\}$ as a function of α for d=1 and several values of r_s. The solid, dashed, dotted, dash-dotted, dash-dot-dotted lines are corresponding to r_s=0.5, 1.5, 3.0, 5.0 and 20.0, respectively.

The effect of the density imbalance $\alpha \equiv (n_e - n_h)/(n_e + n_h)$ on $\Delta_{\max}$ is shown in Fig. 4. It is evident to find that density imbalance actually suppresses $\Delta_{\max}$ and that it has different effects on two sides of the crossover. In the BEC regime, the main effect of the density imbalance reduces the number of electron-hole pairs, which results in that the superfluid properties are less sensitive to density imbalance. In the BCS regime, the density imbalance leads to the mismatch of the Fermi surfaces of electrons and holes and the finite momentum pairing, which is easier to be broken. However, comparing to that in the traditional semiconductor bilayers, we find that the superfluid property in the BEC phase in our case is more sensitive to electron-hole density imbalance. As an example, for r_s=20 the maximum of gap function $\Delta_{\max}$ for TIB disappears at α taking a value smaller than 0.5, while it always takes finite values at α varies in the whole the zone $(-1, 1)$ for the traditional semiconductor electron-hole bilayers [7].

Now we apply this TIB model to study the condensation of electron-hole pairs for the topological surface states of the Bi_2Se_3 material. The two TI films in the left panel of Fig. 1 now are two ultrathin TI Bi_2Se_3 films [20] (about 80 Å thick). With the adopted experimental lattice constants [21] a=4.143 Å and c=28.636 Å, we calculate the first-principles surface band structure of Bi_2Se_3 [22] by a simple supercell approach with spin-orbit coupling included and obtain the approximate Hamiltonian form describing the gapless surface states of Bi_2Se_3 as following,

$$H(\mathbf{k}) = \gamma k^2 + \hbar v_F \left(k_x \sigma_y - k_y \sigma_x\right). \tag{8}$$

Although this Hamiltonian has the same form as that of the conventional two-dimensional electron gas (2DEG) system with Rashba spin-orbit coupling, the intrinsic difference between these two kinds of systems is that the k-linear spin-orbit interaction is primary to the TI surface states, while the parabolic term is dominant in the conventional 2DEG. By fitting the first-principles results, the parameters in Eq. (8) are given as γ=0.21 eV nm^2 and $\hbar v_F$=0.2 eV nm (namely, v_F=3.04×10^5m/s). That means the energy dispersion around the Dirac point can be accurately described by $\epsilon_{\mathbf{k}}$=$\pm\hbar v_F|\mathbf{k}|$ when the wave-vector $|\mathbf{k}|$ is much smaller than 1.0 nm^{-1}. For numerical calculation, we choose nm as the length unit and 0.2 eV as the energy unit throughout this paper. The dielectric constant ε=1 and the spacer width d=10 Å. In fact, the condition that the wave-vector $|\mathbf{k}|$ is much smaller than 1.0 nm^{-1} requires that only for $r_s \geq 5$, then the TIB model is valid for Bi_2Se_3 material. This means that only the BEC phase can most probably emerge in the Bi_2Se_3 bilayer.

Now, let us discuss the critical temperature of this TIB system. The relation between the maximum value $\Delta_{\max}$=max$\{\Delta_{\mathbf{k}}\}$ and temperature T is respectively shown in Fig 5 (a) for d=1, α=0, and several values of

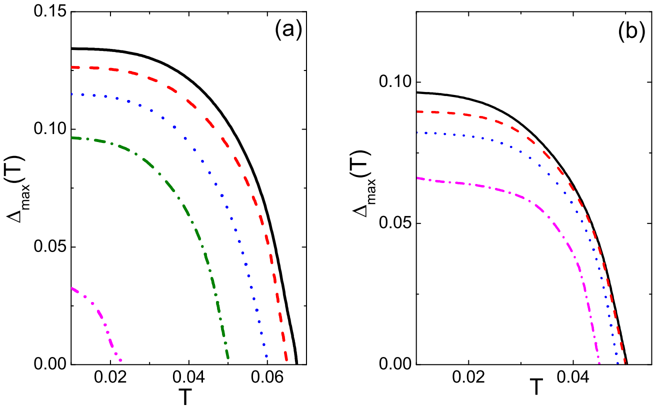

FIG. 5: (Color online) (a) Maximum value $\Delta_{\max}$=max$\{\Delta_{\mathbf{k}}\}$ vs temperature T for d=1, α=0, and several values of r_s. The solid, dashed, dotted, dash-dotted, dash-dot-dotted lines are corresponding to r_s=0.6, 1.5, 3.0, 5.0, and 20.0, respectively. (b) $\Delta_{\max}$ as a function of the temperature T at r_s=5. The solid, dashed, dotted, and dash-dotted lines are corresponding to α=0, 0.05, 0.1, and 0.2, respectively.

r_s, and (b) d=1, r_s=5.0, and several values of α. From Fig. 5(a), we can find that the critical temperature T_c decreases as increasing r_s (i.e., decreasing the particle density). For the Bi$_2$Se$_3$ bilayer at r_s=5.0, the critical temperature T_c is calculated as 0.05 in units of 0.2 eV. That means the critical temperature T_c is about 8$\sim$10 meV (namely, about 100 K), which is much higher than that in the traditional semiconductor electron-hole bilayers. Although the Bi$_2$Se$_3$ TIB system is in the BEC phases (r_s=5.0, 20.0), the numerical calculated results shown in Fig. 5(a) are consistent with the general relation of BCS superconductor,

$$\frac{2\Delta(0)}{T_c} = 2\pi e^{-\gamma} \approx 3.53, \tag{9}$$

where $\Delta(0)$ is the energy gap at zero temperature. The introduced electron-hole density imbalance ($\alpha\neq 0$) can reduce the critical temperature. This character is clearly shown in Fig. 5(b): by increasing the density imbalance α, the critical temperature T_c decreases.

As it is known that in two dimensional superfluids, the critical temperature is often substantially overestimated by mean-filed theory. It is ultimately limited by entropically driven vortex and antivortex proliferation at the Kosterlitz-Thouless (KT) transition temperature $T_{\rm KT}$=$\frac{\pi}{2}\rho_s(T_{\rm KT})$ with $\rho_s(T)$ being the superfluid density (the phase stiffness). We can calculate the superfluid density by the method of evaluating the couterflow current, which is similar to that in Ref. [9]. The superfluid density dependence of temperature is shown in Fig. 6 at r_s=5 and α=0. From Fig. 6, it is evident to estimate that the KT transition temperature $T_{\rm KT}$ is about 0.05 in units of 0.2 eV. Comparing with the critical temperature T_c in Fig. 5 at r_s=5 and α = 0, the striking conclusion is reached: $T_c\approx$ $T_{\rm KT}$, which means that the 100K high-temperature excitonic condensation may occur in the Bi$_2$Se$_3$ TIB system. On the other hand, we can estimate the KT temperature with the zero-temperature phase stiffness $\rho_s(T{=}0)\approx E_F/4\pi$ which is similar with the graphene bilayers [9]. Considering the case shown in Fig. 2, the Fermi energy E_F can be numerical calculated and is given as about 0.4 (in units of 0.2 eV). Hence, the KT temperature is estimated as $T_{\rm KT}\approx E_F/8\approx 0.05$ in units of 0.2 eV. Thus, the two estimated methods are consistent and the 100 K high-temperature excitonic condensation may be protected in the Bi$_2$Se$_3$ TIB system.

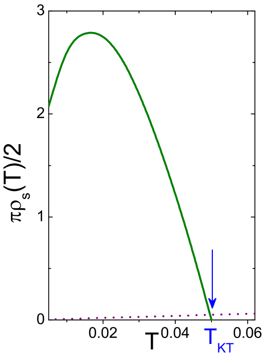

FIG. 6: (Color online) The calculated T_{KT} at r_s=5 and α=0.

IV. CONCLUSION

In summary, we perform a generic TIB model to study the excitonic condensation with the SCMF theory for the topological surface states. Similar to the traditional semiconductor electron-hole bilayers, the TIB system presents the crossover behavior from the BCS in weak coupling limit to Bose-Einstein BEC in the strong coupling limit in zero temperature limit by changing the exciton's density. However, two prominent novel characters different from the traditional semiconductor electron-hole bilayers are found. One is that the superfluid property in the BEC phase is more sensitive to electron-hole density imbalance. The other is that the BCS phase is more robust than that of the semiconductor bilayer in weak coupling limit. Applying this TIB model into Bi$_2$Se$_3$ material, we find that only the BEC phase can be observed in experiment. Moveover, we theoretically estimate the critical temperature for the Bi$_2$Se$_3$ TIB system and find that it is much higher than that in the traditional semiconductor electron-hole bilayers. For example, at r_s=5 and α=0, the critical temperature T_c is obtained as about 100 K. We also study the phase stiffness and find that the KT transition does not suppress the critical temperature for Bi$_2$Se$_3$ in SCMF approximation.

Acknowledgments

This work was supported by NSFC under Grants No. 90921003, No. 10904005 and No. 60776063, and by the National Basic Research Program of China (973 Program) under Grant No. 2009CB929103.

---

[1] D.W. Snoke and J.P. Wolfe, Phys. Rev. B **39**, 4030 (1989); D.W. Snoke, J.P. Wolfe, and A. Mysyrowicz, Phys. Rev. B **41**, 11171 (1990); K.E. O'Hara, L.O. Suilleabhain, and J.P. Wolfe, Phys. Rev. B **60**, 10565 (1999).

[2] T. Hakioğlu and M. Şahin, Phys. Rev. Lett. **98**, 166405 (2007).

[3] X. Zhu, P.B. Littlewood, M.S. Hyberetsen, and T.M. Rice, Phys. Rev. Lett. **74**, 1633 (1995).

[4] C.-H. Zhang and Yogesh N. Joglekar, Phys. Rev. B **77**, 233405 (2008).

[5] Y. Barlas, R. Côté, J. Lambert, and A.H. MacDonald, Phys. Rev. Lett. **104**, 096802 (2010).

[6] C. Comte and P. Nozieres, J. Phys. Paris 43, 1069 1982 ; P.Nozieres and C. Comte, ibid. 43, 1083 1982 .

[7] P. Pieri, D. Neilson, and G.C. Strinati, Phys. Rev. B **75**, 113301 (2007).

[8] M. Ali Can and T. Hakioglu, Phys. Rev. Lett. **103**, 086404 (2009).

[9] H. Min, R. Bistrizer, J.-J. Su, and A.H. MacDonald, Phys. Rev. B **78**, 121401(R) (2008).

[10] B. Seradjeh, H. Weber, and M. Franz, Phys. Rev. Lett. **101**, 246404 (2008).

[11] C.L. Kane and E.J. Mele, Phys. Rev. Lett. **95**, 146802 (2005).

[12] B.A. Bernevig, T.L. Hughes, and S.C. Zhang, Science **314**, 1757 (2006).

[13] M. König, S. Wiedmann, C. Brüne, A. Roth, H. Buhmann, L.W. Molenkamp, X.-L. Qi, and S.-C. Zhang, Science **318**, 766 (2007).

[14] L. Fu and C.L. Kane, Phys. Rev. B **76**, 045302 (2007).

[15] D. Hsieh, D. Qian, L. Wray, Y. Xia, Y.S. Hor, R.J. Cava, and M.Z. Hasan, Nature (London) **452**, 970 (2008).

[16] H.J. Zhang, C.X. Liu, X.L. Qi, X. Dai, Z. Fang, and S.C. Zhang, Nat. Phys. **5**, 438 (2009).

[17] Y. Xia, D. Qian, D. Hsieh, L. Wrayl, A. Pal1, H. Lin, A. Bansil, D. Grauer, Y.S. Hor, and R.J. Cava, Nat. Phys. **5**, 398 (2009).

[18] Y.L. Chen, J.G. Analytis, J.H. Chu, Z.K. Liu, S.K. Mo, X.L. Qi, H.J. Zhang, D.H. Lu, X. Dai, and Z. Fang, Science **325**, 178 (2009).

[19] C.-Z. Chang, K. He, L.-L. Wang, X.-C. Ma, M.-H. Liu, Z.-C. Zhang, X. Chen, Y.-Y. Wang, and Q.-K. Xue, arXiv: 1012.5716 (2010).

[20] T. Hirahara, Y. Sakamoto, Y. Takeichi, H. Miyazaki, S. Kimura, I. Matsuda, A. Kakizaki, and S. Hasegawa, Phys. Rev. B **82**, 155309 (2010).

[21] S. Nakajima, J. Phys. Chem. Solids **24**, 479 (1963).

[22] Z. Wang, Z.-G. Fu, S.-X. Wang, and P. Zhang, Phys. Rev. B **82**, 085429 (2010).